# A Vibration Budget for Observatory Equipment

**Douglas G. MacMartin[a,b] and Hugh Thompson[b]**
[a]Computing + Mathematical Sciences, California Institute of Technology, 1200 E. California Blvd., Pasadena, CA 91125
[b]TMT Observatory Corp., 1111 S. Arroyo Parkway, Suite 200, Pasadena CA 91105

**Abstract.** Vibration from equipment mounted on the telescope and in summit support buildings has been a source of performance degradation at existing astronomical observatories, for adaptive optics performance in particular. Rather than relying only on best practices to minimize vibration, we present here a vibration budget that specifies allowable force levels from each source of vibration in the observatory (e.g., pumps, chillers, cryocoolers, etc.). This design tool helps ensure that the total optical performance degradation due to vibration is less than the corresponding error budget allocation, and is also useful in design trade-offs, specifying isolation requirements for equipment, and tightening or widening individual equipment vibration specifications as necessary. The vibration budget relies on model-based analysis of the optical consequences that result from forces applied at different locations and frequencies, including both image jitter and primary mirror segment motion. We develop this tool here for the Thirty Meter Telescope, but hope that this approach will be broadly useful to other observatories, not only in the design phase, but for verification and operations as well.

## 1 Introduction

Vibration due to equipment both on and off the telescope is a source of potential performance degradation, for adaptive optics (AO) observations in particular. Vibration impacts performance at most operating observatories; see for example the comprehensive review by Kulcsár *et al*[1] – this issue has been a challenge for many years.[2] For the Thirty Meter Telescope (TMT), the error budget allocates 30 nm for the residual AO-corrected rms wavefront error (WFE) due to all vibration sources, including wavefront errors due to both image jitter and M1 segment motion. This is significantly better than what is typically achieved at existing observatories, and will require careful attention during final design and construction.

Efforts are being made to reduce the impact of vibration on delivered AO performance by changing the AO control algorithm[3–5] without changing the vibration environment; similar approaches are being explored for interferometer OPD control.[6] Passive or active damping can also be used to change the structural response to vibration,[7] this changes the vibration environment without changing sources of vibration. And isolation or source relocation can be used to modify source levels directly.[8] All of these are important components of an overall strategy to reach an acceptable and cost-effective solution. However, during the design phase it is invaluable to have a systematic design tool that can be used to levy requirements on subsystems, allow design trades, and track status relative to the top-level performance requirement. Tracking performance with an error budget is standard practice in any observatory design; this *vibration budget* serves a similar role.

To ensure that TMT will deliver acceptable AO image quality despite equipment vibration, we thus place requirements on source amplitudes (in Newtons) for every significant potential source

of vibration. This in turn will affect design decisions such as locating sources off telescope where possible, selecting well-balanced low-vibration equipment, and defining isolation requirements. This design tool will also be used during acceptance and verification of subsystems to ensure that the vibration environment of the telescope is acceptable as built and minimize the potential for costly diagnostics and fixes during operations. Furthermore, we anticipate that the vibration budget will be maintained for the lifetime of the observatory both for ensuring that new equipment meets requirements, and to aid in diagnosis should the vibration environment change.

Our basic approach is to (i) use the telescope finite element model to evaluate the optical sensitivity to forces applied at different locations and at different frequencies, (ii) use this sensitivity analysis to place requirements on all significant sources of vibration so that if these subsystem requirements are met, the vibration contribution to the error budget is met, and (iii) evaluate potential vibration sources to determine what steps (e.g., isolation) would be needed to meet these requirements. We intend to complement this model-based approach with transfer-function measurements made using calibrated sources as the observatory is built; initial measurements at Subaru Observatory are described in [9]. Improved estimates for force levels from different sources will be used to reallocate force budgets to achieve the most cost-effective solution.

Note that in many applications, the vibration environment is specified in terms of the power spectrum of acceleration. However, while this is appropriate to determine, for example, isolator requirements for some sensitive instrument that is mounted in such an environment, it is not sufficient to ensure that such an acceleration power spectrum is met – that requires placing force requirements on sources.

The key analysis here is the modeling of optical sensitivity described in Section 2, including contributions from both image jitter (tip/tilt) and higher-order terms due to motion of the 492 primary mirror segments at TMT; preliminary results can also be found in [10, 11]. The current vibration budget is given in Table 2 in Section 3. The specification applies to the rms force level in Newtons for each source after passing through a filter that has unit gain from 5–20 Hz, but falls off above and below this frequency range. This allows for higher forces at either higher or lower frequency where the AO performance is less sensitive; the shape of the filter is motivated from the modeling described in Section 2. Note that many of the details given here are specific to TMT, including some of the source locations selected for analysis, the quantitative results for the sensitivity to vibration at those locations, and the chosen allocation of forces that make up the budget. However, we present the vibration budget here because we believe that this new methodology will be valuable to other observatories, particularly during the design and construction phases, but potentially during operations as well.

## 2 Sensitivity analysis

We consider the following input locations for vibration forces, also illustrated in Fig. 1. This is clearly not a complete list, but captures most of the larger sources of potential vibration, and gives a representative collection to illustrate the variation in sensitivity to forces at different locations.

1. Pier forces (applied uniformly at the base of the azimuth track). Note that all off-telescope sources affect the optical response through motion of the pier; the propagation of forces from the enclosure or facilities building is not included in the Finite Element Model (FEM) but is captured by an estimated attenuation factor anchored from data taken at Subaru Observatory[9] (see Fig. 7).
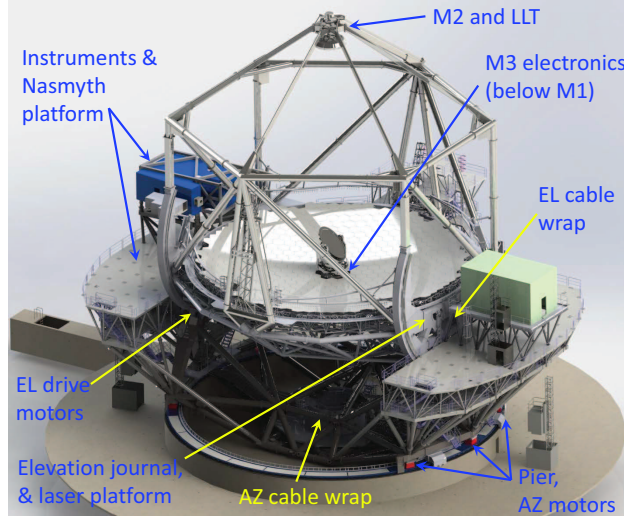
**Fig 1** Force input locations considered for evaluating optical sensitivity to vibration for the Thirty Meter Telescope (TMT).

2. Instruments and other sources on the Nasmyth platforms. Input forces have been considered at all instrument mass nodes and on the Nasmyth platform itself; the response is similar and results are shown here only for forces at one instrument (MIRES).

3. Azimuth and Elevation cable wraps; these are modeled as torques about the respective drive axes. For consistency with other inputs, the response is given per Newton of force, using the cable-wrap radius to scale the moment arm.

4. Laser launch telescope (LLT) and other sources near M2.

5. Sources mounted on the elevation journals; for TMT this includes M2 electronics and the lasers; the latter are mounted on the elevation journal with electronics mounted on a platform attached to the journal.

6. M3 electronics, at the base of the M3 tower. M1 electronics boxes are distributed under the primary mirror, but the optical sensitivity is assumed to be similar to the central location where M3 electronics are placed.

7. Elevation axis direct drive motor on the azimuth structure.

8. Azimuth axis direct drive motor; these forces affect the system similarly to pier forces with one caveat noted below.

The last five locations are potential sources of vibration through the use of cooling fluid, which may exert forces from fluid turbulence that may be difficult to isolate. Vibration forces may also enter the structure at mounting brackets for the pipes carrying cooling fluid (the flow may be turbulent or include pressure fluctuations from compressors/pumps); as the routing of these has not been established, the vibration budget uses sensitivities from representative locations in the list above. For each source location other than cable wrap torques and the telescope pier, the response is calculated for forces in each axis ($F_x$, $F_y$, and $F_z$), and the sensitivities shown in Figure 6 calculated as the rms over all three axes. Sources off the telescope are typically isolated and create only vertical forces; these excite the pier predominantly through the propagation of surface

Rayleigh waves with the resultant vertical motion roughly 50% higher than the horizontal.[12] To capture this effect, we weight the vertical direction 50% higher relative to horizontal in computing the sensitivity to pier and off-telescope forces, but use an equal weighting to compute the sensitivity to forces at the azimuth drive itself.

Vibration caused by sources such as bearing roughness, torque ripple or other actuator noise within the M2 or M3 subsystems overwhelmingly results in local motion of the respective optical surface rather than vibration propagation through the structure.[11] These disturbances apply equal and opposite torques to the telescope structure and the relevant optic; while the former can result in excitation of telescope resonances and motion of other optical surfaces, the resulting image motion is negligible compared with the direct response of the driven surface. There is thus no need to consider these inputs with the full structural model. For TMT, these sources are separately categorized in the error budget as "control noise" and are managed by the relevant subsystem directly.

Forces on the telescope structure and pier result in both image jitter and M1 segment dynamic motion. We predict these effects using two separate models, since different fidelity is required.

The image jitter prediction combines the telescope FEM with a linear optical model and the mount control system (which only affects results at low frequencies). Structural damping of 0.5% is assumed, and the first 4000 modes of the telescope structure are included (up to 50 Hz). A 15 Hz Type-II rejection is included for simulating the residual AO-corrected wavefront error from telescope image motion; the relatively low bandwidth results from the requirement of high sky coverage, combined with the need for natural guide stars for tip/tilt estimation. Seeing-limited performance is also calculated. TMT uses the normalized point-source sensitivity (PSSN), related to rms image jitter $\theta_{\mathrm{rms}}$ as $\mathrm{PSSN} = 1 - \alpha\theta_{\mathrm{rms}}^2$ where $\alpha = 9.12 \times 10^{-6}$ for $\theta_{\mathrm{rms}}$ in mas.

Modeling to predict M1 segment motion model additionally includes a low-order model of the segment dynamics for all 492 primary mirror segments, including the stiffness and internal resonances of the segment support assembly, actuator dynamics that include the actuator servo characteristics, and the global control loop that uses feedback of edge-sensors to maintain segment positions. This model and the control loops are described in more detail in [13]. Note that TMT has selected (soft) voice-coil actuators for control of M1 segment motion, with stiffness at low frequencies provided by a roughly 8 Hz servo loop.[13] Above this frequency, these actuators serve to isolate segment motion from mirror cell motion, greatly reducing the contribution of M1 segment motion to the AO-corrected wavefront error, as illustrated in Figure 2. It is this improvement that drove the selection of soft actuators. Again, both AO-corrected rms wavefront error and PSSN for seeing-limited observations are computed from the M1 segment motion.

The wavefront error from segment motion is partially corrected by the deformable mirrors of the AO system, limited by both the finite temporal bandwidth and spatial fitting errors. These are separately computed here. A 60 Hz bandwidth ($f_c$) is used for temporal correction of M1 segment motion by the AO system; at frequency $f$ the temporal rejection multiplies the spatially-correctable pattern by $S(f) = f/\sqrt{f^2 + f_c^2}$, where $S = 1$ yields no correction and $S = 0$ perfect correction. The spatial fitting error is similarly described by $A(f)$; this is the residual fraction of the amplitude that would remain if the spatial pattern was quasi-static. This factor is calculated using 2-dimensional spatial filtering; this approach is validated for one vibration source to adequately match a comprehensive AO simulation using MAOS.[14] At each frequency, the uncorrected and corrected wavefront errors are computed for two phases of the waveform that are 90° apart; the temporal rms over one full period of the sinusoidal waveform can be obtained from the response
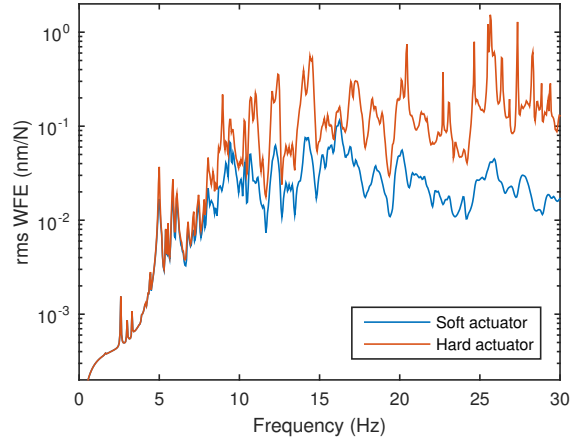
**Fig 2** Comparison of the AO-corrected rms WFE due to the M1 segment motion that results from vertical forcing at the telescope pier if the M1CS actuators were hard (e.g., piezoelectric) or soft (voice-coil, TMT baseline); both the spatial- and temporal correctability are included. Above the 8-10 Hz bandwidth of the actuator servo loop the soft actuators isolate the mirror surface from the motion of the mirror cell; at 30 Hz the reduction relative to an undamped hard actuator is more than a factor of 10.
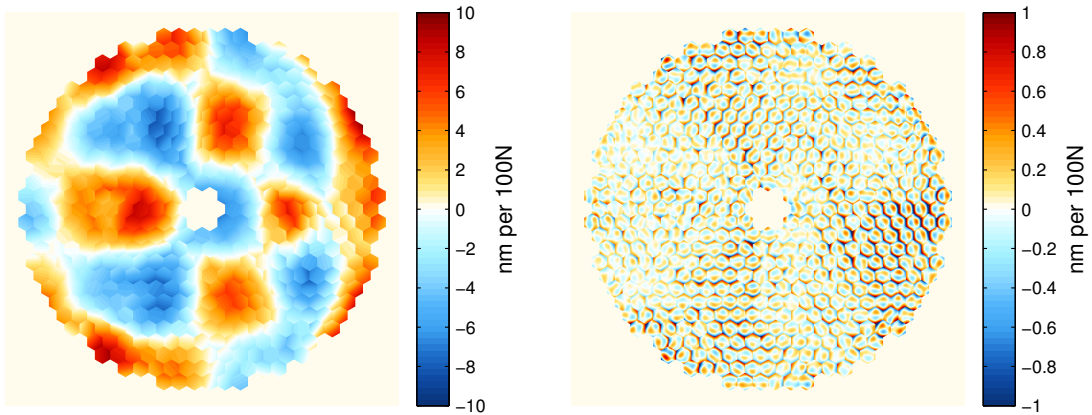


**Fig 3** Representative pattern of M1 segment motion at 30 Hz without (left) and with (right) AO spatial correction; note the different scale. The latter case includes only quasi-static spatial fitting errors (as if the temporal bandwidth were infinite) to illustrate that the spatial pattern of wavefront error is well-corrected by AO, and correction is limited primarily by the temporal AO bandwidth.
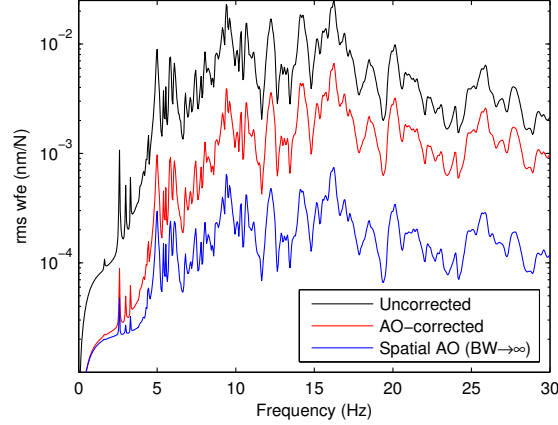
**Fig 4** (Maybe). Wavefront error from M1 segment motion in response to 1 N vertical force on the pier before and after AO correction; also shown is the spatial correctability (as if the temporal bandwidth were infinite); consistent with Fig. 3, this illustrates that the response pattern is spatially well-corrected, but correction is limited by the temporal bandwidth.

at these two phases. Taking into account both temporal and spatial effects, the the net reduction factor that multiplies the rms uncorrected wavefront error is $R = 1 - (1 - A)(1 - S)$. The spatial fitting error is generally small compared with the temporal fitting error from the limited bandwidth because the spatial pattern of M1 response is relatively smooth: even at 30 Hz, where the temporal correctability only reduces spatially-correctable motion by a factor of two ($S \sim 0.5$), then 95% of the motion is spatially correctable ($A \sim 0.05$; Figure 3). The length-scales of M1 motion are determined primarily by mirror cell dynamics rather than the specific source (that is, the factor $A$ is largely independent of where forces are applied). This length scale is roughly consistent with the length-scales of M1 segment motion inferred from AO DM data at Keck.[15]

The combination of soft voice-coil actuators for M1 and the lower AO-rejection bandwidth for tip/tilt means that the residual AO-corrected wavefront error is dominated by image jitter, particularly above 10 Hz; this is illustrated in Fig. 5. Above roughly 10 Hz, the image jitter is typically dominated by motion of M2; overall telescope motion and M1 tip/tilt are important contributors to image jitter below 10 Hz.

The combined AO-corrected wavefront error per Newton of force is shown in Figure 6 for the locations described earlier. For each source location other than cable wrap torques and pier forces, the AO-corrected performance is comptued for forces in each direction ($x$, $y$, $z$) and the rms over the three directions shown. A key observation is that the most sensitive frequency range for vibration forces is typically 5–20 Hz. At lower frequencies, AO rejection is sufficiently good that the sensitivity decreases rapidly with decreasing frequency; there is also no dynamic amplification from telescope structural resonances below 5 Hz. At sufficiently high frequency, inertial effects similarly result in a rapid decrease in sensitivity with increasing frequency. For simplicity, we thus (i) define a single sensitivity for each source location as the rms WFE per Newton over this 5–20 Hz band and (ii) define a frequency-dependent shaping filter that allows for higher forces at
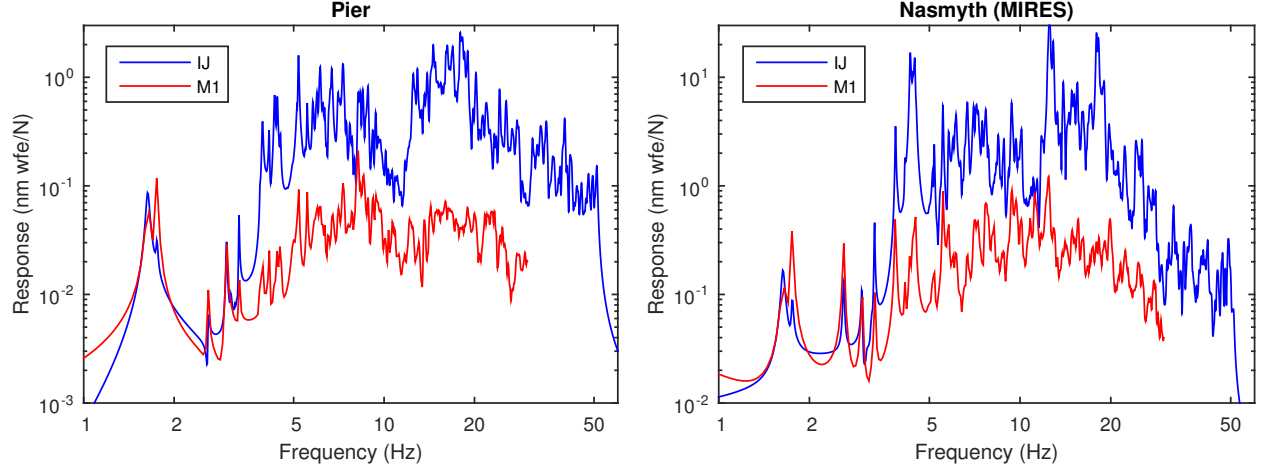
**Fig 5** Contribution to residual AO-corrected wavefront error from image motion and from M1 segment motion for force input at telescope pier (left) and an instrument (right). The M1 contribution is typically less important than image jitter, particularly above 10 Hz, due in part to the choice of soft M1CS actuators and in part to increasing AO tip/tilt rejection at lower frequencies.

higher or lower frequencies. This shaping filter is given by

$$
W(f) = \begin{cases} (f/f_0)^2 & f \leq f_0 \\ 1 & f_0 \leq f \leq f_1 \\ (f/f_1)^{-2} & f \geq f_1 \end{cases}
$$

This is shown with the average sensitivity are shown in Fig. 6. The sensitivity is summarized for each source location in Table 1. Note that the rms WFE is extremely sensitive to several on-telescope locations in particular.

Forces in the facilities building or enclosure result in WFE only through the resulting pier motion, with some additional attenuation of vibration through the soil/pier. Based on data collected at Subaru Observatory, we conservatively estimate that a force in the facilities building results in a factor of at least 10 times less response than a force applied at the telescope pier, and a force at the enclosure pier results in a factor of 5 times less response (see Fig. 7 and [9]).

The discussion above focuses on the AO performance rather than seeing-limited performance. If force levels from equipment are sufficiently low for the former to be acceptable, then the latter performance will also be acceptable. Sensitivities are also provided in Table 1; any force allocation that meets the AO requirement will yield PSSN of roughly 0.9999. A representative PSSN calculation is shown in Figure 8. Unlike for AO, the M1 contribution is typically larger than the image jitter contribution to PSSN, due to the higher spatial-frequency content.

## 3 Vibration Budget

The vibration budget is intended to provide an initial force allocation to each subsystem or source of equipment vibration that helps ensure that the overall error budget allocation to equipment vibration is met. The vibration budget is constructed from the sensitivities estimated earlier and a subjective estimate of the level of difficulty of meeting force requirements for different sources.
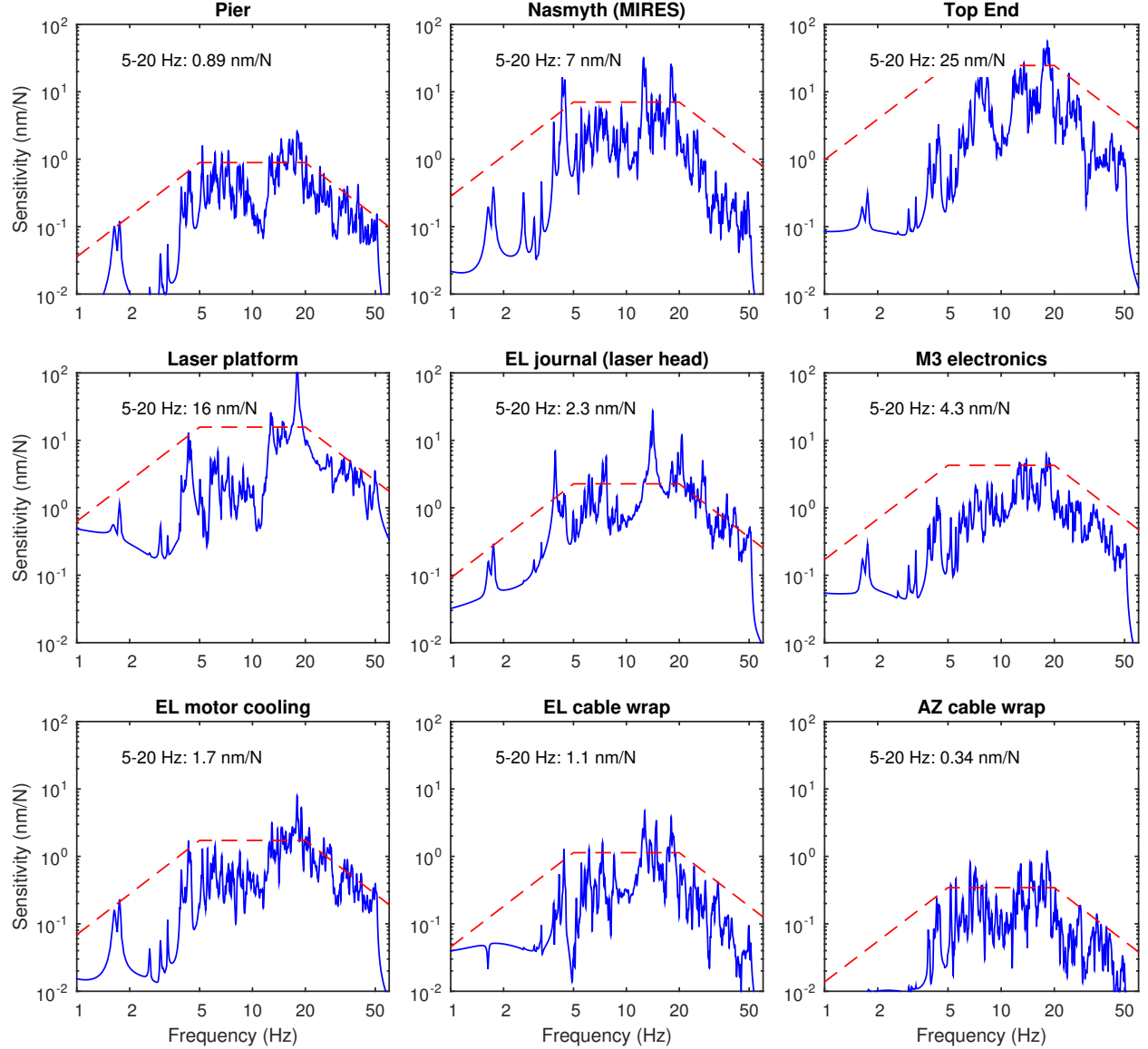
**Fig 6** Sensitivity in nm of AO-corrected wavefront error per Newton of applied force as a function of frequency for forces at the locations given at the beginning of Section 2. For each location, the response is computed due to image motion; the contribution due to M1 segment motion is only included for selected locations. With the exception of the pier and cable wrap inputs, the combined wavefront error plotted is the rms over forces in $x$, $y$, and $z$ directions. Also shown is the "shaping filter" used to approximate the sensitivity, and the average sensitivity over the 5–20 Hz range.

8

| Source | AO Sensitivity (nm/N) | | | PSSN ($N^{-1}$) | | |
|---|---|---|---|---|---|---|
| | IJ | M1 | Combined | IJ | M1 | Combined |
| Facilities Building* | 0.09 | 0.005 | 0.09 | 0.026 | 0.024 | 0.029 |
| Enclosure Pier* | 0.18 | 0.01 | 0.18 | 0.05 | 0.05 | 0.058 |
| Telescope Pier | 0.89 | 0.05 | 0.89 | 0.26 | 0.24 | 0.29 |
| Instruments and Nasmyth platform | 0.38 | 7.0 | 7.0 | 1.0 | 2.0 | 2.3 |
| Laser platform (laser electronics) | 15.6 | 1.9 | 15.7 | 2.2 | 4.5 | 5.0 |
| EL journal (Laser head, M2 electronics) | 2.26 | 0.15 | 2.27 | 0.3 | 0.86 | 0.91 |
| Top end (LGSF, M2 cell) | 24.5 | 0.66 | 24.5 | 2.6 | 3.1 | 4 |
| M3, M1 electronics | 4.26 | 0.2 | 4.27 | 0.6 | 0.9 | 1.1 |
| Azimuth-axis motor (cooling) | 1.1 | 0.07 | 1.17 | 0.22 | 0.33 | 0.39 |
| Elevation-axis motor (cooling) | 1.72 | 0.1 | 1.73 | 0.22 | 0.51 | 0.56 |
| Azimuth cable wrap | 0.01 | 0.34 | 0.34 | 0.06 | 0.06 | 0.09 |
| Elevation cable wrap | 0.02 | 1.14 | 1.14 | 0.17 | 0.11 | 0.2 |

*estimated

**Table 1** Average sensitivity over 5–20 Hz for forces at the locations given in Section 2, in nm of AO-corrected wavefront error per Newton of applied force (from Fig. 6), and factor $\beta$ such that PSSN=$1 - \beta^2 F^2$. Sensitivities for sources in facilities building or enclosure pier are estimated as the sensitivity due to forces on the telescope pier, divided by a factor of 10 or 5 respectively (see Fig. 7).
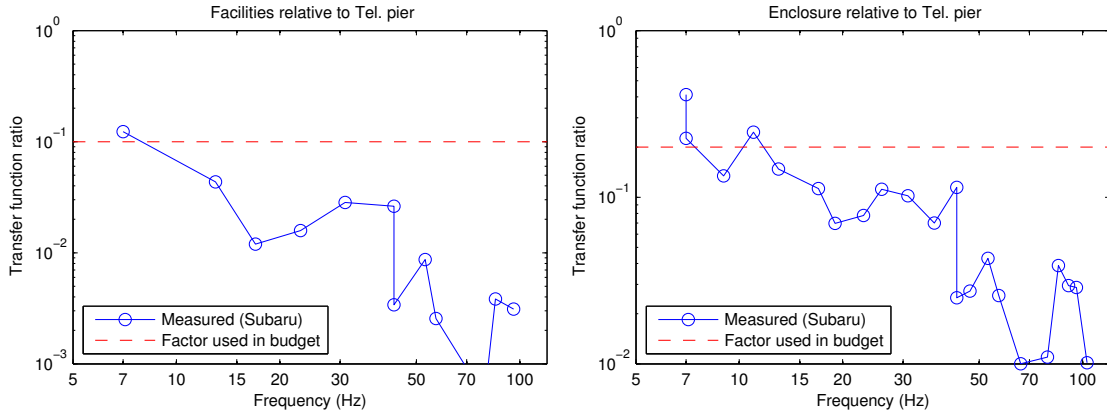


**Fig 7** Ratio of vertical motion on telescope pier due to a force applied on the telescope pier compared with response at the same location due to a force applied in the facilities building (left) or enclosure pier (right). These are measured at Subaru Observatory, using reciprocity to obtain the transfer functions from remote locations. Reduction factors for horizontal motion are comparable. The reduction factors used in constructing the current TMT budget are likely to be conservative except at very low frequency, although of course the soil and pier characteristics differ between the sites.
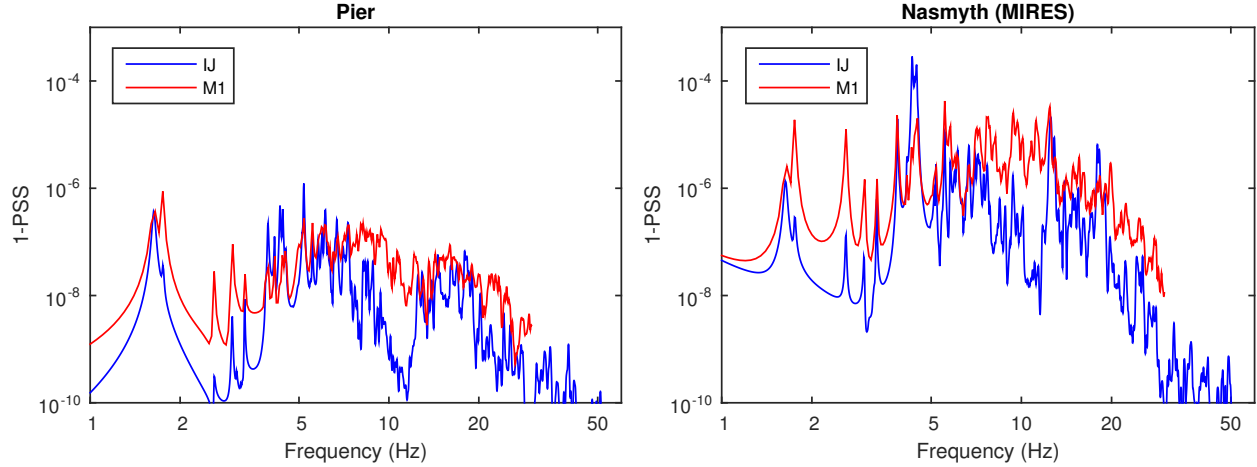
**Fig 8** Contribution to normalized point-source sensitivity (PSSN) from image motion and from M1 segment motion for a one Newton force input at telescope pier (left) and an instrument (right); the PSSN contribution scales quadratically with force. The higher-spatial frequency M1 contribution is typically more important than image jitter.

This is an initial allocation only, which will be revised as further information is available either from design or data.

Our initial allocation is shown in Table 2. For each source, this is the maximum allowable rms force, integrated over all frequencies after passing through the shaping filter described earlier that allows for higher forces at higher or lower frequencies. Individual subsystems can re-allocate between subcomponents within their subsystem. While many of the force allocations appear to be exceptionally small, measurements of some representative equipment suggest that with isolation it may be possible to meet these requirements. For example, the cryopump tested in [9] results in less than 0.04 N rms (after applying the shaping filter) when mounted on 3.6 Hz isolators.

It is clear that the vibration problem is dominated by components at a few locations with particularly high optical sensitivity, including anything at the telescope top-end near M2, the platform supporting the lasers (this may be amenable to redesign), and the Nasmyth platforms. Some large sources of vibration are located in the summit support building (e.g., chillers and pumps associated with the Summit Facilities subsystem, and HSB pumps associated with the telescope structure subsystem). However, because forces in these locations are significantly attenuated through the soil, relatively larger force allocations are allowable.

## 4 Conclusions

Image degradation due to equipment vibration has typically been addressed solely through "best practices" design choices, such as selecting low-vibration equipment, mounting equipment off-telescope where practical, and isolating large vibration sources. While these steps are clearly essential, TMT is establishing requirements on the allowable force levels at different locations in order to ensure that the AO-corrected wavefront errors induced by vibrating equipment remain at acceptable levels, and provide a framework for making cost-effective design choices. This vibration-budget is based on the modeled optical sensitivity resulting from vibrating forces at different locations and different frequencies.

There is clearly substantial uncertainty in predicting the sensitivity of rms WFE to forces as derived herein; the expected force levels from any particular source is also uncertain. Modeling

10

| Subsystem | Subcomponent | Sensitivity (nm/N) | Allowable force (N rms) | Subcomponent AO-WFE (nm) | Aggregate AO-WFE (nm) |
|---|---|---|---|---|---|
| **On Telescope** | | | | | 23.9 |
| Tel. Structure | | | | | 11.1 |
| | Az Drive motor | 1.2 | 1 | 1.2 | |
| | El Drive motor | 1.7 | 1 | 1.7 | |
| | Az Cable wrap | 0.3 | 1 | 0.3 | |
| | El Cable wrap | 1.1 | 1 | 1.1 | |
| | HSB oil distribution | 0.9 | 1 | 0.9 | |
| | Tel. Utility Serv. | 7 | 1.4 | 9.9 | |
| | Other | 4.3 | 1 | 4.3 | |
| M1CS | | 4.3 | 0.5 | 2.1 | 2.1 |
| M2 system | | | | | 5.0 |
| | M2 cell | 24.5 | 0.2 | 4.9 | |
| | M2 electronics | 2.3 | 0.5 | 1.1 | |
| M3 System | | 4.3 | 0.5 | 2.1 | 2.1 |
| Comm. & Info. Systems | | 7.0 | 0.5 | 3.5 | 3.5 |
| LGSF | | | | | 10.0 |
| | Top-end | 24.50 | 0.2 | 4.9 | |
| | BTO | 7.0 | 0.5 | 3.5 | |
| | Lasers | 2.3 | 0.5 | 1.1 | |
| | Laser electronics | 15.7 | 0.5 | 7.9 | |
| Instrumentation cooling | | | | | 9.9 |
| | Cryocooling | 7.0 | 1 | 7.0 | |
| | Refrigerant cooling | 7.0 | 1 | 7.0 | |
| Instruments | | | | | 14.2 |
| | NFIRAOS | 7.0 | 1 | 7.0 | |
| | IRIS | 7.0 | 0.5 | 3.5 | |
| | WFOS | 7.0 | 0.8 | 5.6 | |
| | IRMS/MOSFIRE | 7.0 | 0.5 | 3.5 | |
| | HROS | 7.0 | 0.5 | 3.5 | |
| | IRMOS | 7.0 | 0.5 | 3.5 | |
| | PFI | 7.0 | 0.5 | 3.5 | |
| | MIRAO | 7.0 | 0.5 | 3.5 | |
| | NIRES-B | 7.0 | 0.5 | 3.5 | |
| | NIRES-R | 7.0 | 0.5 | 3.5 | |
| | WIRC | 7.0 | 0.5 | 3.5 | |
| **Within Enclosure** | | | | | 13.2 |
| Enclosure | | 0.18 | 50 | 8.9 | |
| Summit Facilities | | 0.89 | 10 | 8.9 | |
| Tel. Structure | | 0.18 | 10 | 1.8 | |
| Optical cleaning sys. | | 0.18 | 10 | 1.8 | |
| Optical coating sys. | | 0.18 | 10 | 1.8 | |
| Test instruments | | 0.18 | 1 | 0.18 | |
| Optics handling eq. | | 0.18 | 10 | 1.8 | |
| Test instrument ctrl | | 0.18 | 1 | 0.18 | |
| Observatory safety sys. | | 0.18 | 1 | 0.18 | |
| Engineering sensors | | 0.18 | 10 | 1.8 | |
| Comm. & Info. sys | | 0.18 | 1 | 0.18 | |
| **Inside Support Building** | | | | | 10.8 |
| Summit facilities | | 0.09 | 100 | 8.9 | |
| Telescope structure | | 0.09 | 50 | 4.5 | |
| Miscellaneous | | 0.09 | 50 | 4.5 | |

**Table 2** Preliminary vibration budget, giving the allowable force level for each source, and the estimated sensitivity (Table 1) and corresponding AO-corrected wavefront error; the aggregate wavefront error from each subsystem is also given. Many subsystems have equipment in the support building; for clarity these are grouped here under "miscellaneous".

the response of the telescope structure at the frequencies relevant for equipment vibration is challenging and not likely to be highly accurate. Furthermore, it is difficult to estimate unsteady forces from any equipment sources, particularly early in design. However, given the importance of vibration in AO-observations, it is essential that we make the best effort possible with existing tools. We hope that this effort will greatly increase the probability of delivering an observatory without significant vibration-related wavefront errors. We present this tool with the hope that this approach may be a model for other observatories as well.

*References*

1 C. Kulcsár *et al.*, "Vibrations in AO control: a short analysis of on-sky data around the world," in *Proc. SPIE 8447, Adaptive Optics Systems III*, (2012).

2 B. H. Thomas, W. Neville, and J. Snodgrass, "Assessment and control of vibrations affecting large astronomical telescopes," in *Proc. SPIE 732, 1$^{st}$ Intl. Conf. on Vibration control in optics and metrology*, 130–156 (1987).

3 C. Correia, J.-P. Véran, and G. Herriot, "Advanced vibration suppression algorithms in adaptive optics systems," *J. Opt. Soc. Am. A* **29**(3), 185–194 (2012).

4 A. Guesalaga, B. Neichel, F. Rigaut, J. Osborn, and D. Guzman, "Comparison of vibration mitigation controllers for adaptive optics systems," *Applied Optics* **51**(19), 4520–4535 (2012).

5 C. Kulcsár, P. Massioni, G. Sivo, and H.-F. Raynaud, "Vibration mitigation in adaptive optics control," in *Proc. SPIE 8447, Adaptive Optics SYstems III*, (2012).

6 M. Böhm, J.-U. Pott, O. Sawodny, T. Herbst, and M. Kürster, "Real-time vibration compensation for large telescopes," *Monthly Notices of the Royal Astron. Soc.* **442**, 2466–2455 (2014).

7 E. H. Anderson, R. M. Glaese, and D. Neill, "A comparison of vibration damping methods for ground based telescopes," in *Proc. SPIE 7012, Ground-based and airborne telescopes II*, (2008).

8 M. Hess, C. Nance, J. Vause, M. Hrynevych, M. Swain, and M. Colavita, "Strategy for identifying and mitigating facility vibrations to improve optical performance at the W. M. Keck Observatory," in *Proc. SPIE 4837, Large Ground-based Telescopes*, 342–351 (2003).

9 H. Thompson, D. G. MacMartin, P. Byrnes, D. Tomono, and H. Terada, "Measuring transmission and forces from observatory equipment vibration," in *Proc. SPIE 9145, Ground-based and Airborne Telescopes V*, (2014).

10 D. G. MacMartin and H. Thompson, "Development of vibration source requirements for TMT to ensure AO performance," in *Proc., Third AO4ELT Conf.*, (2013).

11 D. G. MacMartin and H. Thompson, "Equipment vibration budget for TMT," in *Proc. SPIE 9145, Ground-based and Airborne Telescopes V*, (2014).

12 H. Lamb, "On the propagation of tremors over the surface of an elastic solid," *Phil. Trans. Royal Soc. A* **203**, 1–42 (1904).

13 D. G. MacMartin, P. Thompson, M. M. Colavita, and M. J. Sirota, "Dynamic analysis of the active-controlled segmented mirror of the Thirty Meter Telescope," *IEEE Trans. Control Sys. Tech.* **22**(1), 58–68 (2013).

14 L. Wang and B. Ellerbroek, "Computer simulations and real-time control of ELT AO systems using graphical processing units," in *Proc. SPIE 8447, Adaptive Optics Systems III*, (2012).

15 D. G. MacMynowski, M. M. Colavita, W. Skidmore, and K. Vogiatzis, "Primary mirror dynamic disturbance models for TMT: Vibration and wind," in *Proc. SPIE 7738, Modeling, Systems Engineering, and Project Management for Astronomy IV*, (2010).